IRI TECHNICAL REPORT 07-01

Use of a genesis potential index to diagnose ENSO effects on tropical cyclone genesis

The International Research Institute for Climate & Society
Earth Institute of Columbia University
Palisades, NY 10964

Cover image from NASA, S115-E-06684 (17 Sept. 2006) --- Hurricane Gordon was captured at 18:15:36 GMT, Sept. 17, 2006 with a digital still camera, equipped with a 20-35mm lens, by one of the crewmembers aboard the Space Shuttle Atlantis. The center of the storm was located near 34.0 degrees north latitude and 53.0 degrees west longitude, while moving north-northeast. At the time the photo was taken, the sustained winds were 70 nautical miles per hour with gusts to 85 nautical miles per hour.

The International Research Institute for Climate and Society (IRI) was established as a cooperative agreement between U.S. NOAA Office of Global Programs and Columbia University.

Use of a genesis potential index to diagnose ENSO effects on tropical cyclone genesis

Suzana J. Camargo[1], *Kerry A. Emanuel* [2] *and Adam H. Sobel*[3]

[1] International Research Institute for Climate and Society,

Lamont Campus, Palisades, NY

[2] Program in Atmospheres, Oceans and Climate,

Massachusetts Institute of Technology, Cambridge, MA

[3] Department of Applied Physics and Applied Mathematics,

and Department of Earth and Environmental Sciences,

Columbia University, New York, NY

Abstract

ENSO (El Niño-Southern Oscillation) has a large influence on tropical cyclone activity. The authors examine how different environmental factors contribute to this influence, using a genesis potential index developed by Emanuel and Nolan. Four factors contribute to the genesis potential index: low-level vorticity (850hPa), relative humidity at 600hPa, the magnitude of vertical wind shear from 850 to 200hPa and potential intensity (PI). Using monthly NCEP Reanalysis data in the period of 1950-2005, we calculate the genesis potential index on a latitude strip from 60° S to 60° N. Composite anomalies of the genesis potential index are produced for El Niño and La Niña years separately. These composites qualitatively replicate the observed interannual variations of the observed frequency and location of genesis in several different basins. This justifies producing composites of modified indices in which only one of the contributing factors varies, with the others set to climatology, to determine which among the factors are most important in causing interannual variations in genesis frequency. Specific factors that have more influence than others in different regions can be identified. For example, in El Niño years, relative humidity and vertical shear are important for the reduction in genesis seen in the Atlantic basin, and relative humidity and vorticity are important for the eastward shift in the mean genesis location in the western North Pacific.

1. Introduction

Understanding the influence of large-scale environmental factors on tropical cyclogenesis is a problem of great scientific and societal importance. While much is known about which factors influence genesis, a quantitative theory is lacking. In the absence of such a theory, empirical methods are useful. Gray (1979) developed an index which was able to replicate key features of the seasonal and spatial variability of observed genesis using a handful of environmental parameters. Such an index is useful in several ways. First, it provides an empirical quantification of the relative contributions of various environmental factors towards genesis. Second, it may conceivably be useful in developing schemes for forecasting tropical cyclone (TC) number, to the extent that an independent capability exists to forecast the large-scale environmental variables which enter the index.

Here, we present another genesis index, and construct composites of it with respect to both the annual cycle and the El Niño - Southern Oscillation (ENSO) phenomenon. Our first goal is to evaluate the ability to represent observed variations of tropical cyclone number with the annual cycle and ENSO in various basins. These are fair tests of the index, since the index was constructed with only climatological information for each hemisphere as a whole. The test of the ability of the index to reproduce observed ENSO signals is perhaps the first one the index must pass in order to be useful for forecasting, since ENSO is the largest single predictable factor influencing genesis in some basins. Our second goal is to use the index to determine which specific environmental factors are most influential in determining ENSO-related variations in genesis in the various basins. The index weights the various factors (sea surface temperature, wind shear, etc.) with specific

functional dependences, which empirically have been found to be appropriate to represent their relative importance in the climatology (and in this study, also to their variability with ENSO). Modified indices were constructed in which all but one factor is set to the climatology, while the interannual variability is retained in the remaining factor. ENSO composites were then constructed for these modified indices, in order to asses the role of each particular factor in ENSO variability. By repeating this procedure for each factor separately and comparing the results, we provide a quantitative basis for stating that one factor is more important than another in inducing the ENSO signal in a given region.

2. Development of the genesis potential index

The genesis potential (GP) index developed by Emanuel and Nolan (2004) was motivated by the work of Gray (1979). Here we describe the development of the index in more detail.

We began with a large set of environmental variables that, on physical grounds, we believed might be important predictors. In selecting combinations of such variables, we avoided the use of parameters that might be specific to the present climate. For example, we did not use a specific threshold for SST (sea surface temperature), as in Gray's index, as we wanted an index that would be valid in different climate scenarios. There are no grounds for believing that 26° C is a constant of nature. Royer et al. (1998) show that the use of this SST threshold limits the validity of Gray's index under climate change.

The initial set of predictors included the potential intensity (Emanuel, 1988), relative humidity,

absolute vorticity at various levels, and wind shear. The wind shear is defined as the magnitude of the vector difference between the horizontal winds at 850 and 200 hPa, as is often used in empirical studies of tropical cyclone genesis and intensity change. While in principle it would be desirable to include as predictors wind shears defined between different levels, the classical definition was retained primarily because satellite cloud-track winds are most abundant in the lower troposphere, where trade-cumulus develop, and near the tropical tropopause, where cirrus clouds are often found.

The predictors were evaluated using the National Centers for Environmental Prediction (NCEP) re-analysis data (Kalnay et al., 1996) from 1950 to 2004. The potential intensity V_{pot} is obtained from sea surface temperature, sea level pressure, and vertical profiles of atmospheric temperature and humidity using a technique which is a generalization of that described in Emanuel (1995) to take into account dissipative heating, as discussed in Bister and Emanuel (1998). Technical details of the calculation of potential intensity may be found in Bister and Emanuel (2002a,b), who also presented some estimates of its climatological, low-frequency variability. A short definition of the potential intensity can be found in Appendix A.

Genesis locations and times were taken from so-called "best track" data sets maintained for the Atlantic and eastern North Pacific by the NOAA National Hurricane Center, and for the rest of the world oceans by the U.S. Navy's Joint Typhoon Warning Center. Only post-1970 data were used. Monthly average values of each of the predictors were then tested individually and in combination for their ability to replicate the annual cycle of tropical cyclogenesis rates in each hemisphere,

as well as for their ability to replicate the spatial distribution of genesis in each month of the year. This process was partly objective, using standard multiple regression techniques, but also partly subjective, in the selection of combinations of variables and the choice of which variables to retain. We make no claim that the resulting index represents a globally optimum combination of the chosen predictors.

The index, as presented by Emanuel and Nolan (2004), is defined

$$GP = \left|10^5\eta\right|^{3/2} \left(\frac{\mathcal{H}}{50}\right)^3 \left(\frac{V_{\rm pot}}{70}\right)^3 (1 + 0.1V_{shear})^{-2} ,$$

where η is the absolute vorticity at 850hPa in s^{-1}, $\mathcal{H}$ is the relative humidity at 600hPa in percent, $V_{\rm pot}$ is the potential intensity in ms^{-1}, and $V_{\rm shear}$ is the magnitude of the vertical wind shear between 850hPa and 200hPa in ms^{-1}. Aside from the coefficient multiplying the shear, the constants that appear in this definition are entirely arbitrary and simply designed to give an index value of order unity. Although the index should be interpreted as a rate per unit time per unit area, a constant multiplier would have to be included in the index to give it the appropriate magnitude and dimensions. In developing the index, its log was fit to the best track data using multiple regression, but experimenting empirically with the shear factor to optimize its fit to the data. The exponents that appear in the index have been rounded to the nearest half integer as the fit to the data does not warrant more precision.

The seasonal genesis index developed by Gray (Gray, 1979; Watterson et al., 1995) has some similarities with GP, but also some important differences. A few of the variables are common

to both indices, such as the vertical wind shear (though using different pressure levels) and the midtropospheric relative humidity. Other variables are somewhat equivalent; for example, while here the absolute low-level vorticity is one of the factors, in Gray's index, the Coriolis parameter and the relative vorticity are separate variables. The main difference between these indices is in the thermodynamic variable. GP uses the potential intensity, which depends on the air-sea thermodynamic disequilibrium and the difference between the sea surface temperature and the temperature at the level of neutral buoyancy for an adiabatically lifted boundary layer parcel. In contrast, Gray's index uses the near-surface ocean thermal energy with a specific threshold (26°C) and the vertical gradient of the equivalent potential temperature between the surface and 500hPa.

Besides the difference in variables used, the indices also differ in the powers and constants used in their definitions. Gray's index is able to reproduce approximately the regions of tropical cyclogenesis in the seasons and basins of tropical cyclone activity (see e.g. Watterson et al. (1995)). An alternative modification of the Gray's index to suppress the dependence on the SST threshold using a convective parameter is discussed in Royer et al. (1998). These genesis indices have also been applied to output from climate models (Ryan et al., 1992; McDonald et al., 2005; Chauvin et al., 2006).

In the following section, we compare the spatial and seasonal distributions of genesis events to those predicted by the GP.

3. Climatology of the genesis potential index

Fig. 1 shows the climatological values of the genesis potential in February and September, within the peak of the tropical cyclone season in the southern and northern hemisphere, respectively. In Fig. 2 the annual maximum of the genesis potential climatology at each grid point is shown, with all well known tropical cyclone-prone regions appearing as maxima of the genesis potential index. While the spatial patterns agree well in a qualitative sense, the spatial distributions of genesis potential and genesis itself do not correspond with great quantitative precision.

The annual cycles of genesis events in each hemisphere are shown in Fig. 3 and compared to the predictions using the genesis potential index. The genesis potential captures the main elements of the seasonal cycle of tropical cyclones.

The index was optimized to give the best fit to the spatial and temporal distributions shown in Figures 1 and 3. No attempt was made to optimize the index for variability within individual ocean basins, so it is instructive to evaluate the local performance of the index.

The climatology of the genesis potential per basin (for the definitions of the basins used to compute the area averages, see the caption of table 2), compared with the climatology of the number of tropical cyclones, is shown in Fig. 4 for several basins. The agreement in all basins is very good, with the genesis potential annual cycle's being very similar to that of the number of tropical cyclones. Even in the case of the North Indian Ocean, which has annual cycle with two peaks, pre- and post- monsoon, the genesis potential index follows the number of tropical cyclones very closely.

The average number of tropical cyclones observed over each entire basin varies significantly more, from basin to basin, than does the genesis potential. That is, in Fig. 4, there is more variation in the scale on the left than on the right. It seems reasonable to attribute this in large part to the different size of the basins. The western north Pacific, for example, has a much larger area over which conditions are favorable for genesis than do the other basins. This alone should be expected to lead to a larger number of cyclones in the western north Pacific than the other basins — as is observed — even for the same genesis potential per unit area.

The relationship of the genesis potential index to its four constituent variables (potential intensity, vorticity, vertical wind shear and relative humidity) can be further explored by computing joint probability distribution functions (PDFs) of the index and each of these variables, as shown in Fig. 5. The joint PDFs are estimated from the density of points in the space defined by the index and the other variable, where each point represents the values from an individual grid point in the climatology. All ocean points from 40°S-40°N and all seasons are used. These PDFs show that, in the aggregate over all basins, the different variables play somewhat similar roles in determining the climatological distribution of the index. The index has a threshold-like dependence on potential intensity, wind shear, and relative humidity; there are essentially no large values of the index if shear is large or either relative humidity or potential intensity is small. The density of points at very small values of the index and either large potential intensity, large relative humidity,or small shear is also small compared to that at small values of the index and either small potential intensity, small relative humidity, or large shear. Absolute vorticity does not seem to exhibit threshold

behavior at any finite value, though the index does tend to increase with absolute vorticity (as we expect from its construction). The index can also be low when absolute vorticity is high, as in extratropical regions with low potential intensity. The impression one has is that a favorable value of one constituent variable can compensate for an unfavorable value of another to some degree, allowing the index to attain a fairly large value, with the exception that high values of absolute vorticity cannot compensate if the other variables are unfavorable.

Analogous plots using individual basins (not shown) are qualitatively similar, though details differ somewhat from basin to basin, reflecting modest variation in the way the different variables combine to determine the climatological structure of the genesis potential index. We will show below that different variables are important in generating the ENSO signals in the index in different basins.

4. ENSO and tropical cyclone activity

The influence of ENSO on tropical cyclone activity in the various basins has been studied by a large number of investigators. Recent reviews of this subject may be found in Landsea (2000) and Chu (2004).

In the Atlantic, in El Niño years, there is a tendency toward fewer tropical cyclones, while the opposite occurs in La Niña years (Gray, 1984; Gray and Sheaffer, 1991; Gray et al., 1993; Knaff, 1997). ENSO also affects the number of landfalls in the U.S. (Bove et al., 1998; Pielke Jr. and Landsea, 1999), hurricane intensity (Landsea et al., 1999) and genesis location (Elsner and Kara,

1999). Factors that have been identified as responsible for this shift in tropical cyclone activity are vertical wind shear (Shapiro, 1987; Goldenberg and Shapiro, 1996) and thermodynamic variables (Tang and Neelin, 2004).

In the western North Pacific, there is a southeastward (northwestward) shift of tropical cyclone activity in El Niño (La Niña) years (Chan, 1985; Dong, 1988; Chia and Ropelewski, 2002; Wang and Chan, 2002). This has been attributed to the eastward extension of the monsoon trough and westerlies in the western North Pacific (Lander, 1994, 1996) and reduction of vertical wind shear (Clark and Chu, 2002). In El Niño years typhoons also tend to last longer, become more intense and have more recurved trajectories (Wang and Chan, 2002; Camargo and Sobel, 2005; Camargo et al., 2007), which influences landfall probabilities in Asian countries (Saunders et al., 2000; Elsner and Liu, 2003; Wu et al., 2004). Sobel and Camargo (2005) hypothesized that anomalous typhoon-induced near-equatorial westerly winds generated in El Niño years might even act to strengthen the warm event, resulting in a positive feedback between ENSO and tropical cyclones.

More hurricanes tend to form in the Central Pacific during El Niño events. More tropical cyclones occur near Hawaii. This has been attributed to smaller vertical wind shear and greater low-level relative vorticity in that region (Wu and Lau, 1992; Chu and Wang, 1997; Clark and Chu, 2002; Chu, 2004).

Eastern North Pacific tropical cyclone activity tends to be enhanced when Atlantic tropical cyclone activity is suppressed, and vice-versa (Elsner and Kara, 1999). Although no ENSO influence has been found in tropical cyclone frequency in the eastern North Pacific (Whitney and Hobgood,

1997), the number of intense hurricanes tends to increase in El Niño years (Gray and Sheaffer, 1991) and the tropical cyclone activity shifts westward during El Niño events (Irwin and Davis, 1999), with an increased likelihood that some of these hurricanes will propagate into the central North Pacific (Chu, 2004). This shift has been attributed to environmental parameters' having different characteristics east and west of 116°W (Collins and Mason, 2000) in ENSO years.

There is a strong association between the variabilities of the sea surface temperatures in the Indian and Pacific oceans (Pan and Oort, 1983). The association of North Indian Ocean tropical cyclone frequency and ENSO is apparent during the months of May and November, when fewer intense tropical cyclones occur during El Niño events (Singh et al., 2000).

In El Niño years an increase in the formation of tropical cyclones occurs in the South Pacific near the date line, simultaneously with a decrease near Australia (Revell and Goulter, 1986; Hastings, 1990; Evans and Allan, 1992; Basher and Zeng, 1995). In La Niña years, an enhanced risk of landfall occurs in Australia, with more tropical cyclones tracking close to the Queensland coast, while in El Niño years the tracks are more zonal west of the date line (Nicholls, 1979, 1985; Dong, 1988; Nicholls et al., 1998). This shift is realated to the extension of the monsoon trough and equatorial westerlies in El Niño years in the South Pacific, favoring the formation of twin tropical cyclones (Ferreira et al., 1996), tropical cyclogenesis late in the season and east of 160°W in the South Pacific (Chu, 2004).

5. ENSO influence on the genesis potential index

To assess the environmental factors that determine the ENSO influence on tropical cyclone activity, we begin by calculating the genesis potential index' monthly anomaly (difference from seasonal climatology) in the period 1950-2005. From these anomalies we obtain seasonal anomaly composites for El Niño and La Niña events. We use the Nino3.4 index to define El Niño/La Niña events, considering ASO (August - October) values for the northern hemisphere and JFM (January - March) values for the southern hemisphere. The 13 years (25% of the cases) with the highest (lowest) Nino3.4 values in a season are defined as El Niño (La Niña) years, with the remaining years defined as neutral years, the same definition used in Goddard and Dilley (2005) and Camargo and Sobel (2005). The ENSO years used in the composites for JFM and ASO are given in table 1. Fig. 6 shows these composites for ASO (August - October), the peak period of tropical cyclone activity in the North Atlantic and Western North Pacific.

In Fig. 6(a) the genesis potential anomalies in El Niño years (ASO) show the well known decrease of cyclone activity in the North Atlantic and western part of the western North Pacific (horse shoe pattern), and an increase in the Eastern and Central Pacific. An almost mirror image appears in the La Niña years (Fig. 6(b)), as can be seen especially easily in the difference between El Niño and La Niña years (Fig. 6(c)).

To provide objective observational metrics with which to compare the genesis index, we compute genesis density and track density from best track data. The genesis density is calculated by counting the number of tropical cyclones with genesis (first position) in each $2.5^\circ \times 2.5^\circ$ latitude

and longitude square. Similarly, for the track density, we count the number of six hourly tropical cyclone positions within each $2.5^\circ \times 2.5^\circ$ latitude and longitude square, normalized such that 24 hours in a particular location for one tropical cyclone is counted as one.

The difference in observed ASO genesis and track density anomalies between El Niño and La Niña years is shown in Fig. 7. In the Northern Hemisphere these differences are clearly similar to those exhibited by the genesis potential index anomalies (compare Fig. 6(c) to Fig. 7). The genesis potential index composites in Fig. 6 are able to reproduce the shift in the distribution of Atlantic tropical cyclones between El Niño and La Niña years, for instance. In the next section, we use the genesis potential index to further explore which factors are most responsible for some of these ENSO signals in tropical cyclone activity.

The agreement between observed and predicted El Niño-La Niña differences is not good in the southern hemisphere during ASO. There are very few tropical cyclones in the southern hemisphere during August-October, so this disagreement is not important.

The JFM (January-March) genesis potential ENSO anomalies are shown in Fig. 8 (El Niño (a) and La Niña (b)), together with the difference between the El Niño and La Niña anomalies. The El Niño-La Niña differences in genesis density and track density for JFM are shown in Fig. 9. The ENSO-related shifts are more zonal in the northern hemisphere (though few tropical cyclones form there in JFM) and more meridional in the southern hemisphere. There is also, however, a longitudinal shift in the South Pacific, with a positive genesis potential anomaly in El Niño years east of $160^\circ E$ in the South Pacific and a negative anomaly near the Australian continent.

The genesis potential ENSO anomalies differences in ASO and JFM are generally consistent with the known effects of ENSO on tropical cyclones discussed in the previous section, such as the decrease of tropical cyclone activity in the Atlantic in El Niño years accompanied by an increase in the eastern and central Pacific, with a southeastern shift in the western North Pacific.

Table 2 shows the values of the interannual correlations between the genesis potential index and the number of tropical cyclones in the different basins for different seasons. All basins, with the exception of the North Indian Ocean, have significant skill at least in a few seasons. The western North Pacific has significant correlation in the early and late season, but not during the peak of its tropical cyclone activity, when the Central North Pacific region has significant skill. This shift in skill is probably related to the spatial shift of tropical cyclone activity in the western North Pacific with ENSO. The Atlantic and the eastern North Pacific have significant correlation in the August to October period, when most their peak tropical cyclone activity occurs. In the southern hemisphere, the South Indian and the south Pacific have significant correlations in NDJ (November - January) and DJF (December - February) seasons.

6. Factors influencing ENSO effects on the genesis potential index

Here we assess the individual importance of the four variables that comprise the genesis potential (vorticity, vertical wind shear, potential intensity and humidity) in determining the ENSO anomalies. In order to do this, we recalculate the genesis potential using the long-term climatology of three of the variables but the unmodified, interannually varying values for the fourth variable. This

is then repeated for each of the other three variables. The anomalies and the ENSO composites are then recalculated in all four cases. Due to the nonlinearity of the GP index, the net anomaly cannot be described as the sum of the four fields described here. Nonetheless, to the extent that the index provides weights which appropriately quantify the roles of the different factors in genesis and the nonlinearities are not too large, the attributions obtained by this method should be meaningful.

Fig. 10 shows the El Niño -La Niña difference in genesis potential anomalies for the southern hemisphere in JFM, in the cases of varying (a) vorticity, (b) vertical wind shear, (c) potential intensity, and (d) relative humidity, in each case with the other 3 variables fixed at their long-term climatological values. Comparing this with the pattern obtained when all four factors are varying (Fig. 8(c)), it is apparent that different factors contribute to the genesis potential anomaly shifts in different regions. The increase in the genesis potential anomalies around 10°S is mainly owing to vertical wind shear and vorticity (South Pacific) or vertical wind shear and PI (South Indian). The decrease of the genesis potential anomalies in the South Indian Ocean around 15°S and in the Mozambique channel is mainly owing to vertical wind shear and relative humidity changes. In the South Pacific, from the eastern Australian coast to the east of the date line, the main contribution to the negative genesis potential anomaly is the relative humidity, while east of the date line vertical wind shear and potential intensity dominate the differences. Pattern correlations of the genesis potential anomaly with all factors varying and the genesis potential anomaly with only one factor varying confirm these findings (not shown). For instance, in ASO, the pattern correlations of the GP and the GP with varying vertical wind shear are highly significant in the Atlantic.

Fig. 11 is similar to Fig. 10, but for the northern hemisphere in ASO. For eastern North Pacific, wind shear is the main contributor to the ENSO genesis potential anomalies, with potential intensity also playing a role, and vorticity and relative humidity acting in the opposite sense to the total observed anomaly. In the Atlantic, relative humidity (unfortunately, the variable in which we have the least confidence in the reanalysis) has the strongest contribution, with wind shear also playing a significant role, and potential intensity and vorticity weaker, if not necessarily negligible roles. In the case of the western North Pacific, the negative anomaly near the Asian continent is mainly owing to relative humidity, with an additional contibution from the potential intensity. The increase near the date line is mainly due to vorticity, as claimed previously by Wang and Chan (2002); Chu (2002), with additional contributions from wind shear and relative humidity.

It is interesting to note that the PI anomalies are negative in the western North Pacific in El Niño years, despite the occurrence of more intense typhoons in El Niño years. This is in agreement with the lack of a relationship between local SST in the western North Pacific and tropical cyclone activity in that region (Chan and Liu, 2004; Chan, 2005, 2006). It also supports the notion that the increase in intensity in the WNP during El Niño years is due to the longer lifetimes which occur as a result of the eastward displacement in mean genesis location — that is, over these longer lifetimes, tropical cyclones are able to come closer to their potential intensities. The same explanation was given by Emanuel (2000) for the overall greater intensities of WNP storms compared to Atlantic storms.

In the Indian Ocean, there is a shift of the genesis potential from the northern to the southern

part of the Bay of Bengal, mainly owing to wind shear, which is also mainly responsible for the anomalous positive genesis potential in the Arabian Sea. Though the peak of the tropical cyclone activity in the eastern North Pacific and and North Indian Ocean occurs in JAS and OND, respectively (not shown here), the ASO figures are in agreement with those.

7. Conclusions

We have constructed annual cycle and ENSO composites of an empirical index of tropical cyclone genesis. The index was constructed from only the climatological annual cycle in each hemisphere as a whole, using no information from individual basins, nor any interannual variability whatsoever. Our goals were to test the ability of the index to reproduce observed variations in tropical cyclone activity with the annual cycle and ENSO, and then to use modified versions of the index to determine which individual physical factors are most important in causing these variations.

The primary findings are as follows:

1. The index tracks the observed climatological annual cycles of tropical cyclone number in each individual basin separately.

2. The index successfully reproduces the most well-known ENSO signals in the best-observed basins, such as the suppression of genesis in the Atlantic and the eastward shift in mean genesis location in the western north Pacific during El Niño.

3. The different factors entering the index contribute differently to its ENSO anomalies in dif-

ferent regions. Vertical wind shear and mid-level relative humidity are consistently important in many basins, especially the western North Pacific near the Asian continent, the north Atlantic, and the southern Hemisphere. Vorticity anomalies contribute most significantly in the central Pacific (both north and south), where during El Niño events the tropical cyclones tend to form nearer the equator. Potential intensity plays a secondary role in the Atlantic, and varies oppositely to the observed variations in total genesis potential in the western north Pacific.

Acknowledgements We would like to thank Anthony G. Barnston for valuable discussions. This work was supported in part by NOAA through a block grant to the International Research Institute for Climate and Society. AHS acknowledges support from NSF grant ATM-05-42736.

APPENDIX A

Potential Intensity

The definition of potential intensity is based on that given by Emanuel (1995) as modified by Bister and Emanuel (1998). Details of the calculation may be found in Bister and Emanuel (2002a). The definition is also discussed in http://wind.mit.edu/˜emanuel/pcmin/pclat/pclat.html. A FORTRAN subroutine to calculate the potential intensity is available at http://wind.mit.edu/˜emanuel/home.html. Monthly mean values may be found at http://wind.mit.edu/˜emanuel/pcmin/climo.html. Here we present a very brief overview of Bister and Emanuel (2002a). The formula they use is

$$V_{\rm pot}^2 = \frac{C_k}{C_D}\frac{T_s}{T_0}\left(\mathrm{C}APE^* - \mathrm{C}APE^b\right), \tag{A.1}$$

where C_k is the exchange coefficient for enthalpy, C_D is the drag coefficient, T_s is the sea surface temperature, and T_0 is the mean outflow temperature. The convective available potential energy (CAPE) is the vertical integral of parcel buoyancy, which is a function of parcel temperature, pressure, and specific humidity, as well as the vertical profile of virtual temperature. The quantity CAPE* is the value of CAPE for an air parcel at the radius of maximum winds which has first been saturated at the sea surface temperature and pressure, while CAPE^b refers to the value of CAPE for ambient boundary layer air but with its pressure reduced (isothermally) to its value of at the radius of maximum wind. Thus the variables used to calculate the potential intensity at each grid

point are the sea surface temperature and pressure and vertical profiles of temperature and specific humidity.

References

Basher, R. E. and X. Zeng, 1995: Tropical cyclones in the southwest Pacific - Spatial patterns and relationships to Southern-Oscillation and sea-surface temperature. *J. Climate*, **8**, 1249–1260.

Bister, M. and K. A. Emanuel, 1998: Dissipative heating and hurricane intensity. *Meteor. Atm. Phys.*, **52**, 233–240.

— and —, 2002a: Low frequency variability of tropical cyclone potential intensity, 1, interannual to interdecadal variability. *J. Geophys. Res.*, **107**, 4801, doi:10.1029/2001JD000776.

— and —, 2002b: Low frequency variability of tropical cyclone potential intensity, 2, climatology for 1982-1995. *J. Geophys. Res.*, **107**, 4621, doi:10.1029/2001JD000780.

Bove, M. C., J. B. Elsner, C. W. Landsea, X. Niu, and J. O'Brien, 1998: Effect of El Niño on U.S. landfalling hurricanes, revisited. *Bull. Am. Meteorol. Soc.*, **79**, 2477–2482.

Camargo, S. J. and A. H. Sobel, 2005: Western North Pacific tropical cyclone intensity and ENSO. *J. Climate*, **18**, 2996–3006.

—, A. W. Robertson, S. J. Gaffney, P. Smyth, and M. Ghil, 2007: Cluster analysis of typhoon tracks, Part II: Large Scale Circulation and ENSO, *J. Climate*, in press.

Chan, J. C. L., 1985: Tropical cyclone activity in the Northwest Pacific in relation to El Niño/Southern Oscillation phenomenon. *Mon. Wea. Rev.*, **113**, 599–606.

—, 2005: Interannual and interdecadal variations of tropical cyclone activity over the western North Pacific. *Meteorol. Atmos. Phys.*, **89**, 143–152, doi 10.1007/s00703-005-0126-y.

—, 2006: Comment on "Changes in tropical cyclone number, duration, and intensity in a warming environment". *Science*, **311**, 1713.

— and K. S. Liu, 2004: Global warming and western North Pacific typhoon activity from an observational perspective. *J. Climate*, **17**, 4590–4602.

Chauvin, F., J.-F. Royer, and M. Déqué, 2006: Response of hurricane-type vortices to global warming as simulated by ARPEGE-Climat at high resolution. *Clim. Dyn.*, **27**, 377–399, doi: 10.1007/s00382-006-0135-7.

Chia, H. H. and C. F. Ropelewski, 2002: The interannual variability in the genesis location of tropical cyclones in the Northwest Pacific. *J. Climate*, **15**, 2934–2944.

Chu, P.-S., 2002: Large-scale circulation features associated with decadal variations of tropical cyclone activity over the central North Pacific. *J. Climate*, **15**, 2678–2689.

—, 2004: *Hurricanes and typhoons, past, present and future*, Columbia University Press, New York, chapter ENSO and tropical cyclone activity. 297–332, edited by R. J. Murnane and K.-B. Liu.

— and J. Wang, 1997: Tropical cyclone occurences in the vicinity of Hawaii: Are the differences between El Niño and non-El Niño years significant? *J. Climate*, **10**, 2683–2689.

Clark, J. D. and P.-S. Chu, 2002: Interannual variation of tropical cyclone activity over the Central North Pacific. *J. Meteorol. Soc. Japan*, **80**, 403–418.

Collins, J. M. and I. M. Mason, 2000: Local environmental conditions related to seasonal tropical cyclone activity in the Northeast Pacific basin. *Geophys. Res. Lett.*, **27**, 3881–3884.

Dong, K., 1988: El Niño and tropical cyclone frequency in the Australian region and the North-western Pacific. *Aust. Meteor. Mag.*, **36**, 219–255.

Elsner, J. B. and A. B. Kara, 1999: *Hurricanes of the North Atlantic: Climate and society*. Oxford University Press, New York.

— and K. B. Liu, 2003: Examining the ENSO-typhoon hypothesis. *Clim. Res.*, **25**, 43–54.

Emanuel, K. A., 1988: The maximum intensity of hurricanes. *J. Atmos. Sci.*, **45**, 1143–1155.

—, 1995: Sensitivity of tropical cyclones to surface exchange coefficients and a revised steady-state model incorporating eye dynamics. *J. Atmos. Sci.*, **52**, 3969–3976.

—, 2000: A statistical analysis of tropical cyclone intensity. *Mon. Wea. Rev.*, **128**, 1139–1152.

— and D. S. Nolan, 2004a: Tropical cyclone activity and global climate. *26th Conference on Hurricanes and Tropical Meteorology*, Amer. Meteor. Soc., Miami, FL, 240–241.

Evans, J. L. and R. J. Allan, 1992: El Niño/Southern Oscillation modification to the structure of the monsoon and tropical cyclone activity in the Australian region. *Int. J. Climatol.*, **12**, 611–623.

Ferreira, R. N., W. H. Schubert, and J. J. Hack, 1996: Dynamical aspects of twin tropical cyclones associated with the Madden-Julian oscillation. *J. Atmos. Sci.*, **53**, 929–945.

Goddard, L. and M. Dilley, 2005: El Niño: Catastrophe or opportunity? *J. Climate*, **18**, 651–665.

Goldenberg, S. B. and L. J. Shapiro, 1996: Physical mechanisms for the association of El Niño and West African rainfall with Atlantic major hurricane activity. *J. Climate*, **9**, 1169–1187.

Gray, W. M., 1979: *Meteorology over the tropical oceans*, chap. Hurricanes: Their formation, structure and likely role in the tropical circulation, pp. 155–218, Roy. Meteor. Soc..

Gray, W. M., 1984: Atlantic seasonal hurricane frequency. Part I: El-Niño and 30-MB quasi-biennial oscillation influences. *Mon. Wea. Rev*, **112**, 1649–1688.

— and J. D. Sheaffer, 1991: *Teleconnections linking worldwide anomalies*, Cambridge University Press, New York, chapter El Niño and QBO influences on tropical cyclone activity. 257–284, edited by M.H. Glantz, R.W. Katz and N. Nicholls.

—, C. W. Landsea, P. W. Mielke Jr., and K. J. Berry, 1993: Predicting Atlantic basin seasonal tropical cyclone activity by 1 August. *Wea. Forecasting*, **8**, 73–86.

Hastings, P. A., 1990: Southern Oscillation influences on tropical cyclone activity in the Australian/South-west Pacific region. *Int. J. Climatol.*, **10**, 291–298.

Irwin, R. P. and R. Davis, 1999: The relationship between the Southern Oscillation index and tropical cyclone tracks in the eastern North Pacific. *Geophys. Res. Let.*, **26**, 2251–2254.

Kalnay, E., M. Kanamitsu, R. Kistler, W. Collins, D. Deaven, L. Gandin, M. Iredell, S. Saha, G. White, J. Woollen, Y. Zhu, M. Chelliah, W. Ebisuzaki, W. Higgins, J. Janowiak, K. Mo, C. Ropelewski, J. Wang, A. Leetmaa, R. Reynolds, R. Jenne, and D. Joseph, 1996: The NCEP/NCAR 40-year reanalysis project. *Bull. Amer. Meteor. Soc.*, **77**, 437–441.

Knaff, J. A., 1997: Implications of summertime sea level pressure anomalies in the tropical Atlantic region. *J. Climate*, **10**, 789–804.

Lander, M. A., 1994: An exploratory analysis of the relationship between tropical storm formation in the western North Pacific and ENSO. *Mon. Wea. Rev.*, **122**, 636–651.

—, 1996: Specific tropical cyclone tracks and unusual tropical cyclone motions associated with a reverse-oriented monsoon trough in the western North Pacific. *Wea. Forecasting*, **11**, 170–186.

Landsea, C. W., 2000: *El Niño: Impacts of multiscale variability on natural ecosystems and society*, Cambridge University Press, chapter El Niño-Southern Oscillation and the seasonal predictability of tropical cyclones. 149–181, edited by H. F. Díaz and V. Markgraf.

—, R. A. Pielke Jr., A. M. Mestas-Nuñez, and J. A. Knaff, 1999: Atlantic basin hurricanes: Indices of climatic changes. *Climatic Changes*, **42**, 89–129.

Livezey, R. E., and W. Y. Chen, 1983: Statistical field significance and its determination by Monte Carlo techniques. *Mon. Wea. Rev.*, **111**, 46–59.

McDonald, R. E., D. G. Bleaken, D. R. Cresswell, V. D. Pope, and C. A. Senior, 2005: Tropical

storms: representation and diagnosis in climate models and the impacts of climate change. *Clim. Dyn.*, **25**, 19–36.

Nicholls, N., 1979: A possible method for predicting seasonal tropical cyclone activity in the Australian region. *Mon. Wea. Rev.*, **107**, 1221–1224.

—, 1985: Predictability of interannual variations of Australian seasonal tropical cyclone activity. *Mon. Wea. Rev.*, **113**, 1144–1149.

—, C. W. Landsea, and J. Gill, 1998: Recent trends in Australian region tropical cyclone activity. *Meteor. Atmos. Phys.*, **65**, 197–205.

Pan, Y. H. and A. H. Oort, 1983: Global climate variations connected with sea-surface temperature anomaliesin the eastern equatorial Pacific ocean for the 1958–1973 period. *Mon. Wea. Rev.*, **111**, 1244–1258.

Pielke Jr., R. A. and C. N. Landsea, 1999: La Niña, El Niño and Atlantic hurricane damages in the United States. *Bull. Amer. Meteor. Soc.*, **80**, 2027–2033.

Revell, C. and S. Goulter, 1986: South Pacific tropical cyclones and the Southern Oscillation. *Mon. Wea. Rev.*, **114**, 1138–1144.

Royer, J.-F., F. Chauvin, B. Timbal, P. Araspin, and D. Grimal, 1998: A GCM study of the impact of greenhouse gas increase on the frequency of occurrence of tropical cyclone. *Climatic Change*, **38**, 307–343.

Ryan, B. F., I. G. Watterson, and J. L. Evans, 1992: Tropical cyclone frequencies inferred from Gray's yearly genesis parameter: Validation of GCM tropical climate. *Geophys. Res. Lett.*, **19**, 1831–1834.

Saunders, M. A., R. E. Chandler, C. J. Merchant, and F. P. Roberts, 2000: Atlantic hurricanes and NW Pacific typhoons: ENSO spatial impacts on occurrence and landfall. *Geophys. Res. Lett.*, **27**, 1147–1150.

Shapiro, L. J., 1987: Month-to-month variability of the Atlantic tropical circulation and its relationship to tropical storm formation. *Mon. Wea. Rev.*, **115**, 1598–1614.

Singh, O. P., T. M. A. Khan, and M. S. Rahman, 2000: Changes in the frequency of tropical cyclones over the North Indian ocean. *Meteor. Atmos. Phys.*, **75**, 11–20.

Sobel, A. H and S. J. Camargo, 2005: Influence of western North Pacific tropical cyclones on their environment. *J. Atmos. Sci.*, **62**, 3396–3407.

Tang, B. H. and J. D. Neelin, 2004: ENSO influence on Atlantic hurricanes via tropospheric warming. *Geophys. Res. Lett*, **31**, L24204, doi:10.1029/2004GL021072.

Wang, B. and J. C. L. Chan, 2002: How strong ENSO events affect tropical storm activity over the western North Pacific. *J. Climate*, **15**, 1643–1658.

Watterson, I. G., J. L. Evans, and B. F. Ryan, 1995: Seasonal and interannual variability of tropical cyclogenesis: Diagnostics from large-scale fields, *J. Climate*, **8**, 3052–3066.

Whitney, L. D. and J. Hobgood, 1997: The relationship between sea surface temperature and maximum intensities of tropical cyclones in the eastern North Pacific. *J. Climate*, **10**, 2921–2930.

Wu, G. and N. C. Lau, 1992: A GCM simulation of the relationship between tropical storm formation and ENSO. *Mon. Wea. Rev.*, **120**, 958–977.

Wu, M. C., W. L. Chang, and W. M. Leung, 2004: Impacts of El Niño Southern Oscillation events on tropical cyclone landfalling activity in the western North Pacific. *J. Climate*, **17**, 1419–1428.

List of Figures

(a)

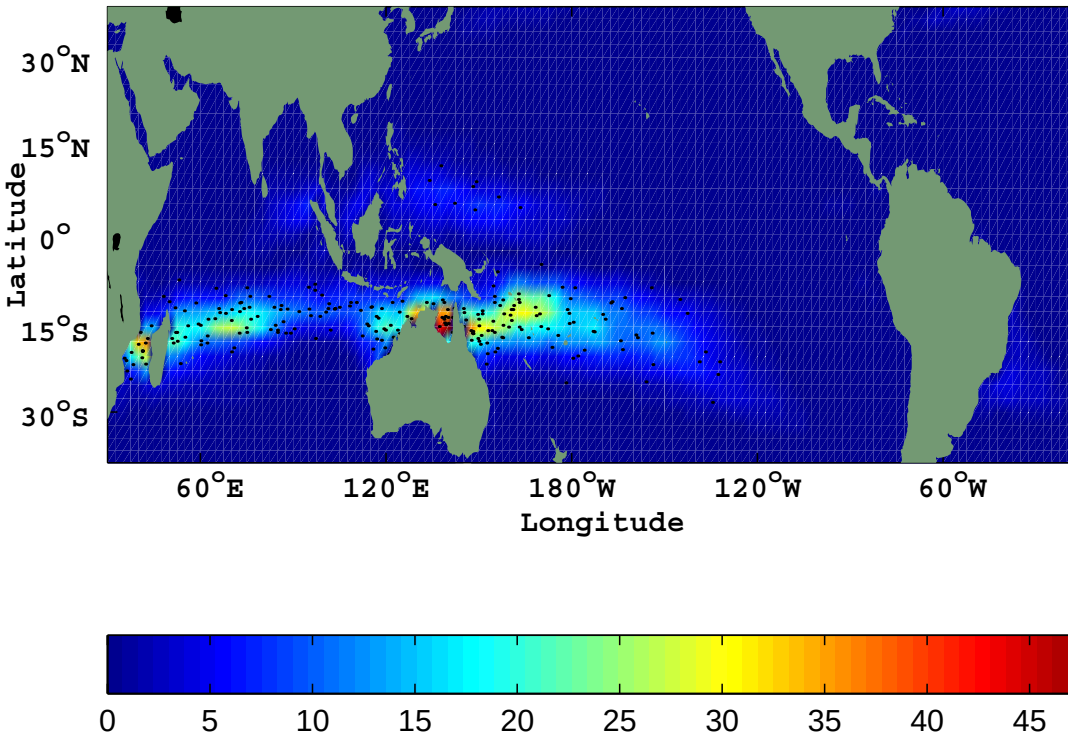

(b)

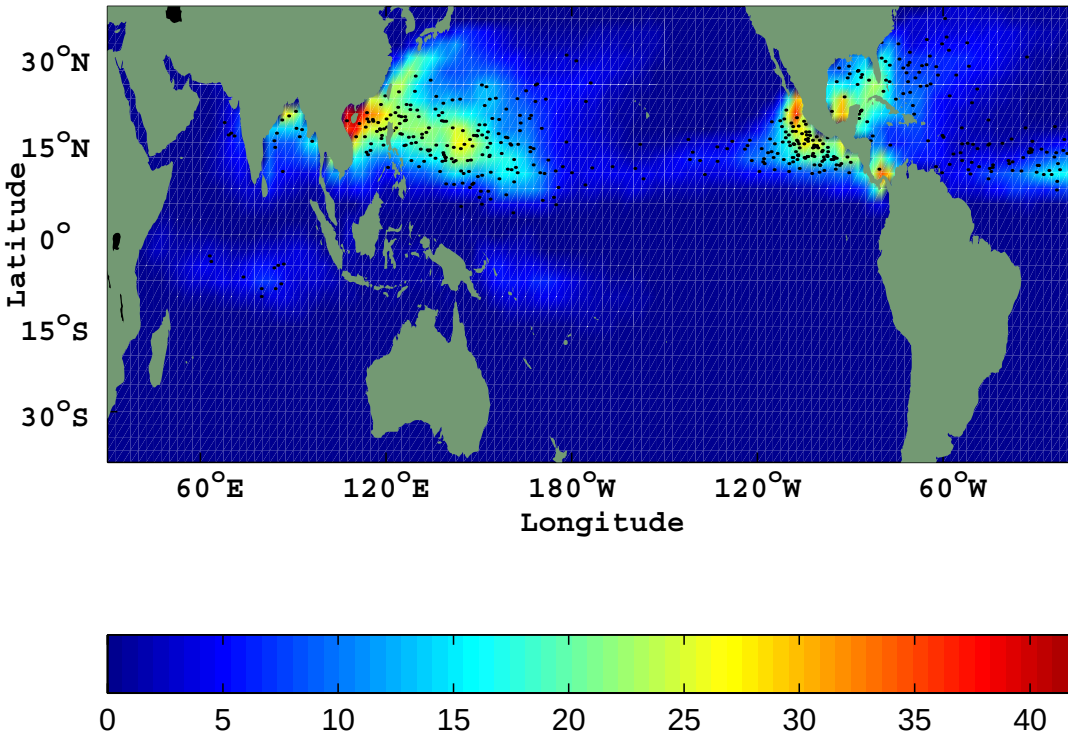

Figure 1: Genesis potential index climatology in February (a) and September (b). The black dots show individual genesis events over the period from 1970-2004 (a) and 1970-2005 (b).

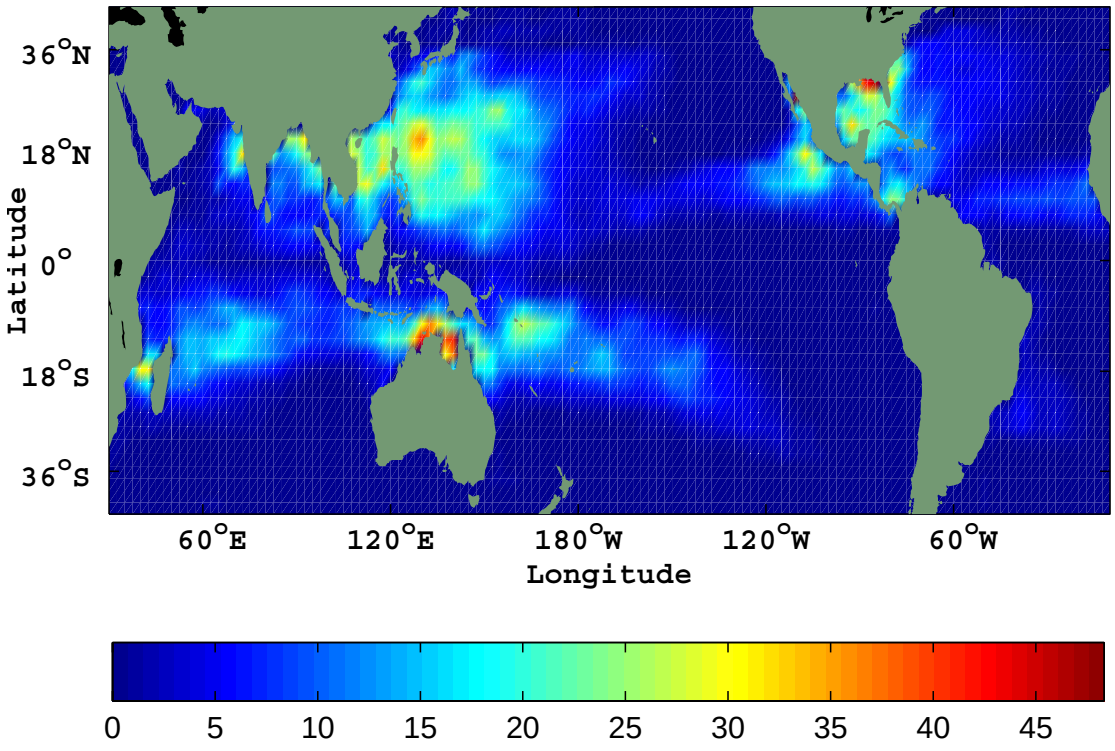

Figure 2: Annual maximum of the genesis potential index climatology at each grid point. The black dots show individual genesis events over the period 1970-2004 (southern hemisphere) or 1970-2005 (northern hemisphere).

(a)

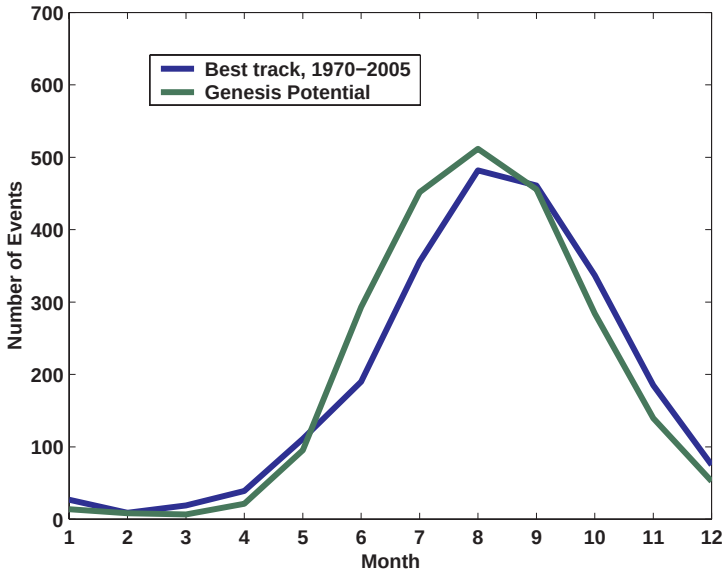

(b)

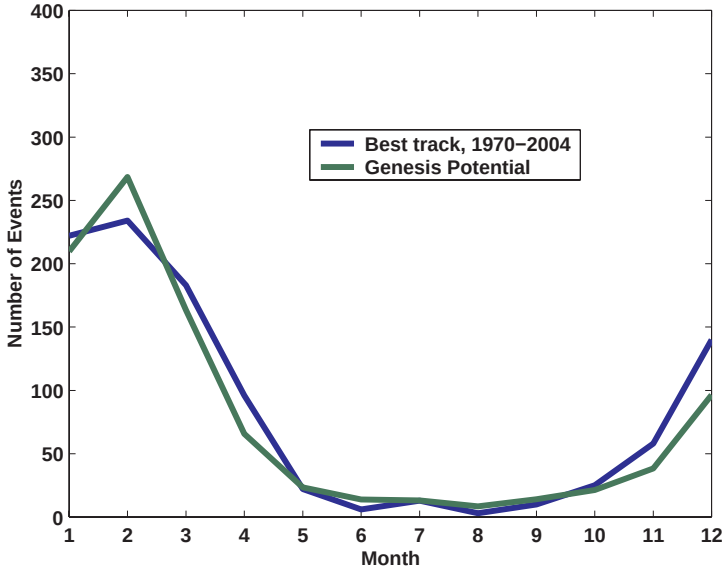

Figure 3: Genesis potential index climatology and number of genesis events in the Northern (a) and Southern (b) hemispheres.

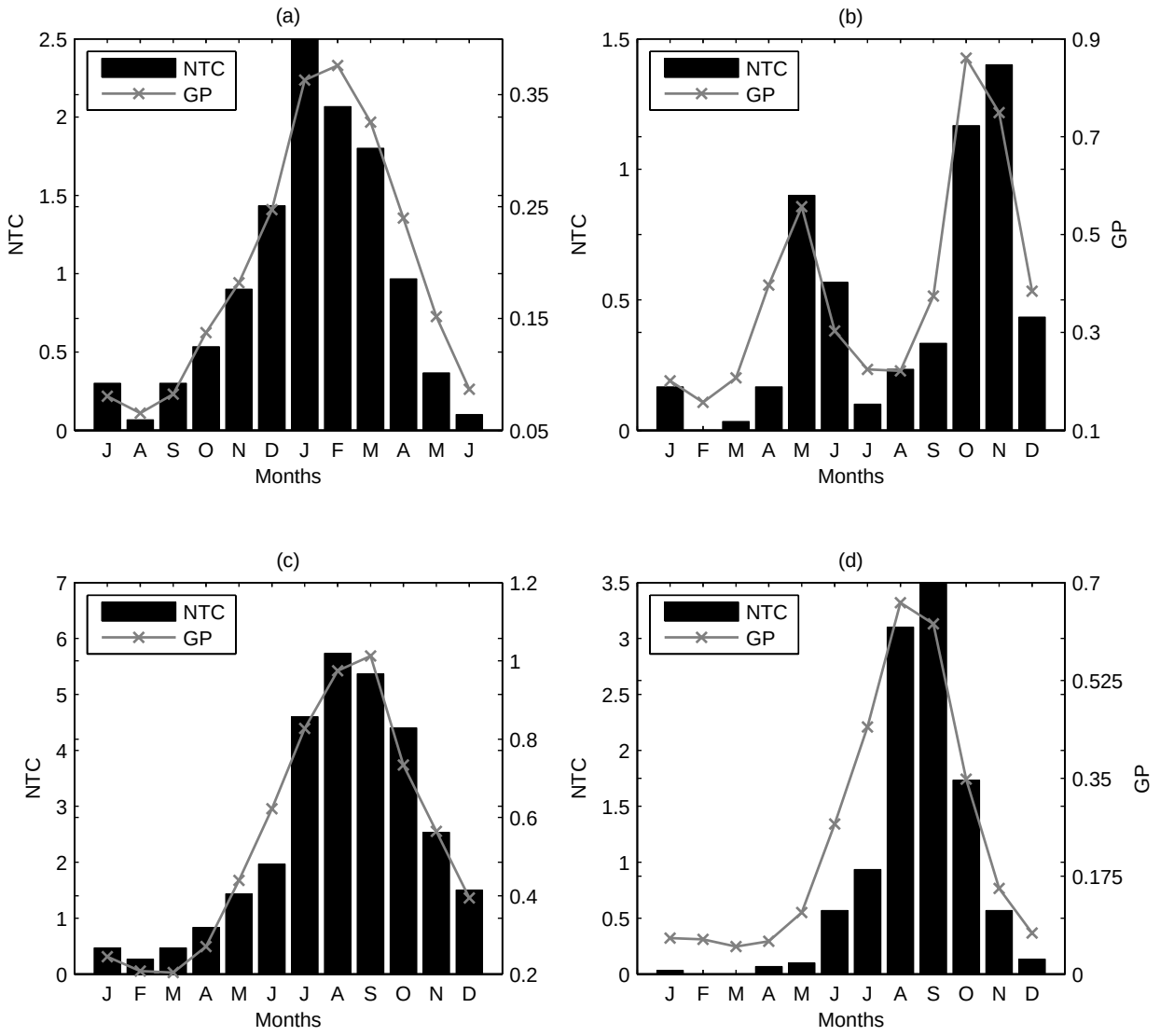

Figure 4: Genesis potential index and climatological number of tropical cyclones in the (a) South Pacific, (b) North Indian, (c) western North Pacific and (d) North Atlantic basins.

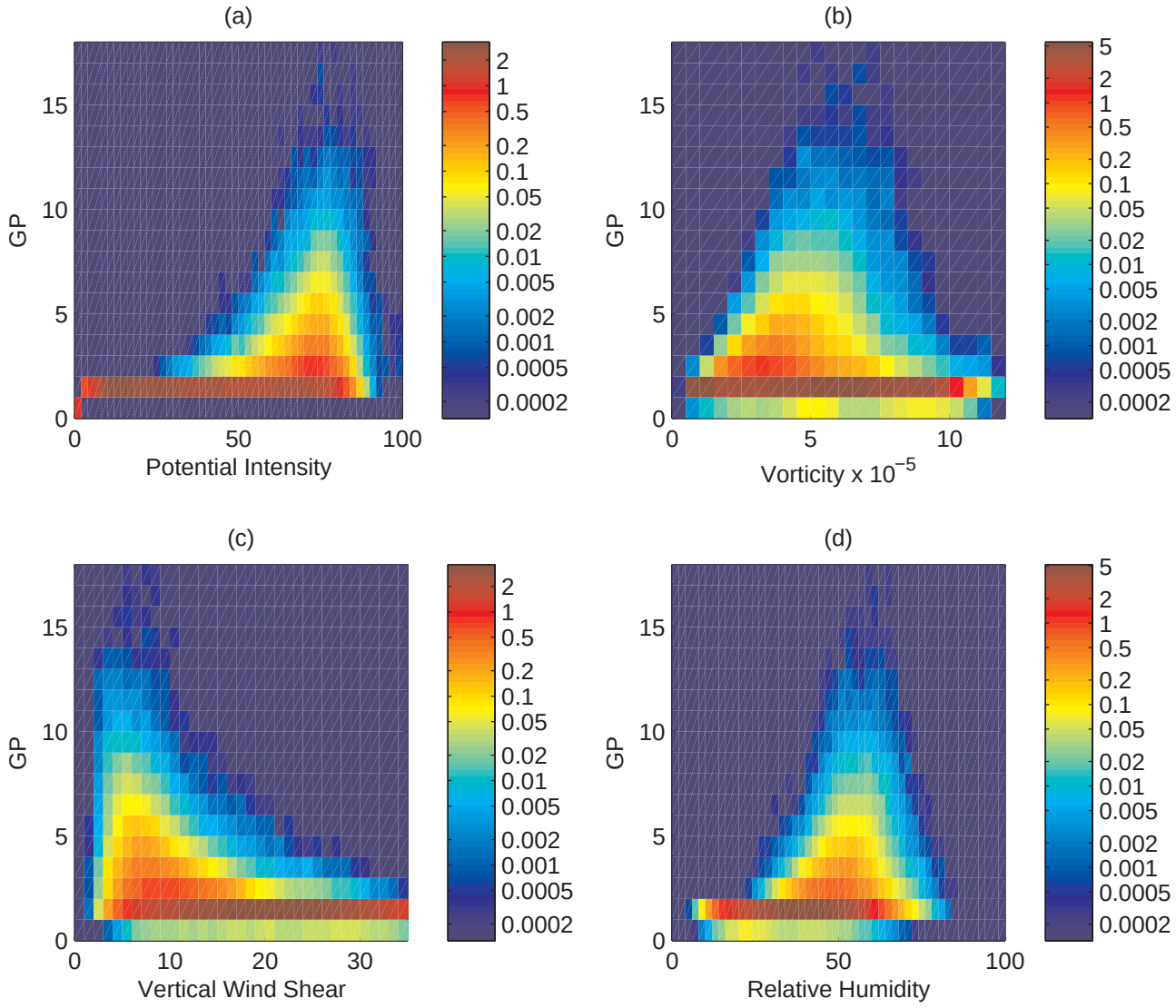

Figure 5: Joint probability distribution functions of the genesis potential index and (a) potential intensity, (b) vorticity, (c) vertical wind shear, and (d) relative humidity for ocean points in the latitude band 40°S - 40°N.

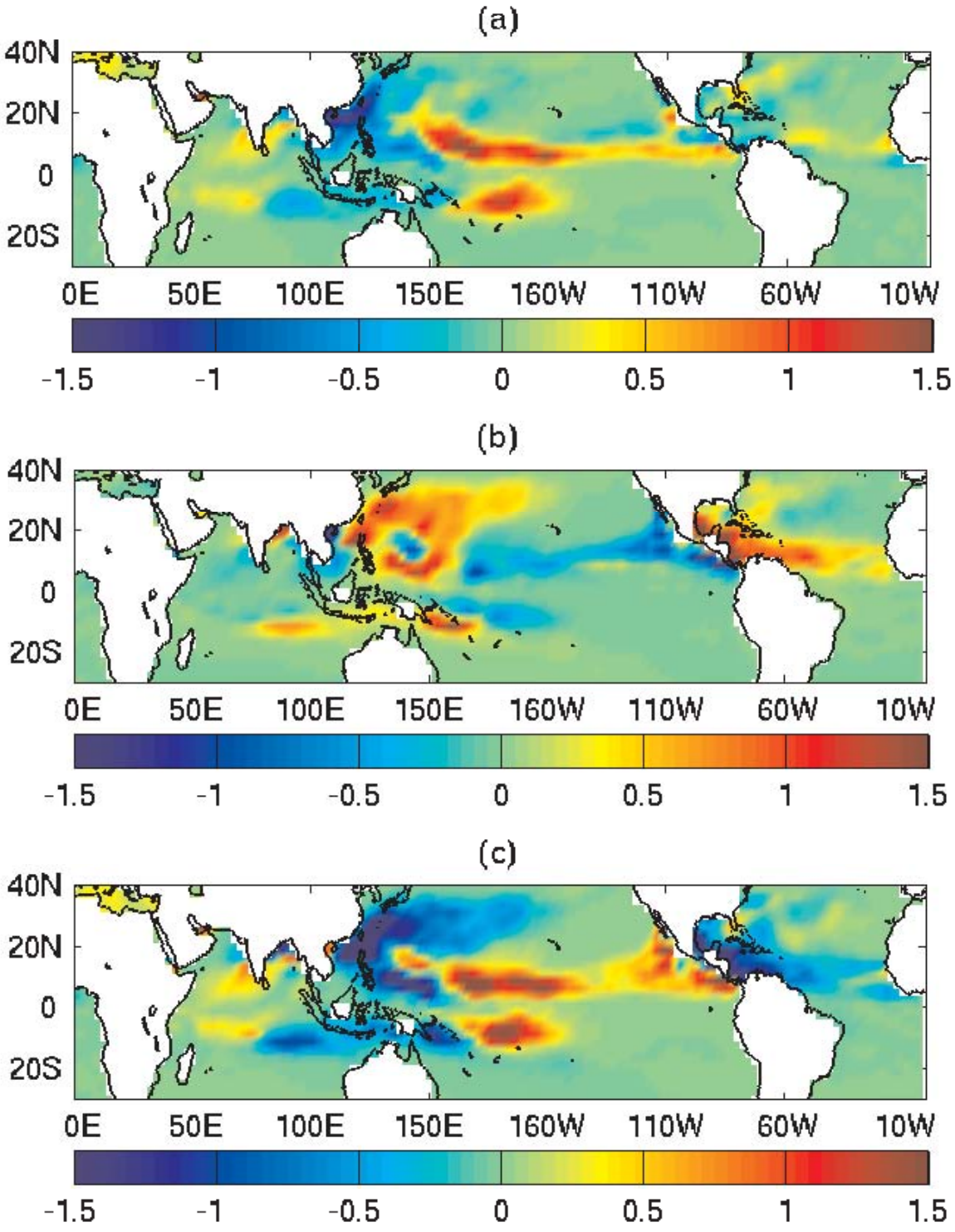

Figure 6: Genesis potential anomalies in ASO (August-October) for (a) El Niño and (b) La Niña years; (c) difference of the anomalies in El Niño and La Niña years.

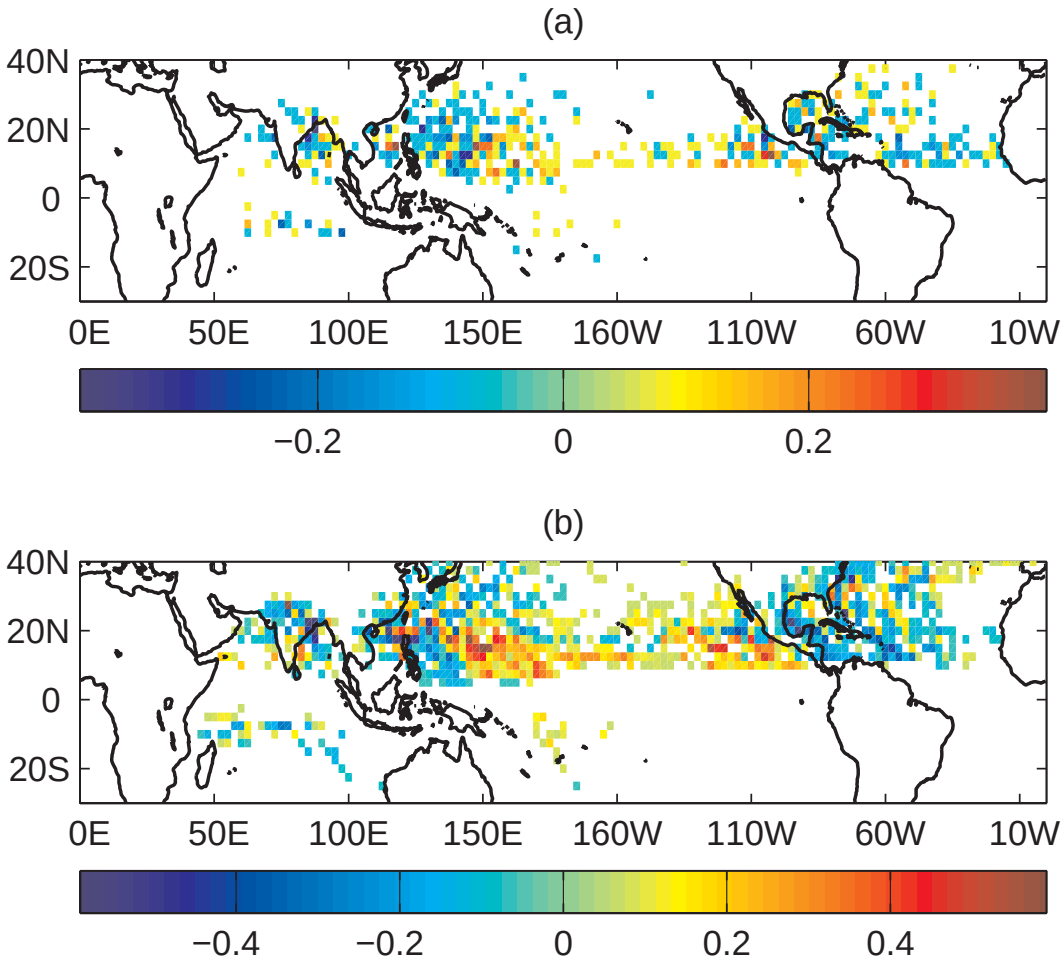

Figure 7: Difference between anomalies in El Niño and La Niña years of the genesis density (a) and track density (b) in ASO.

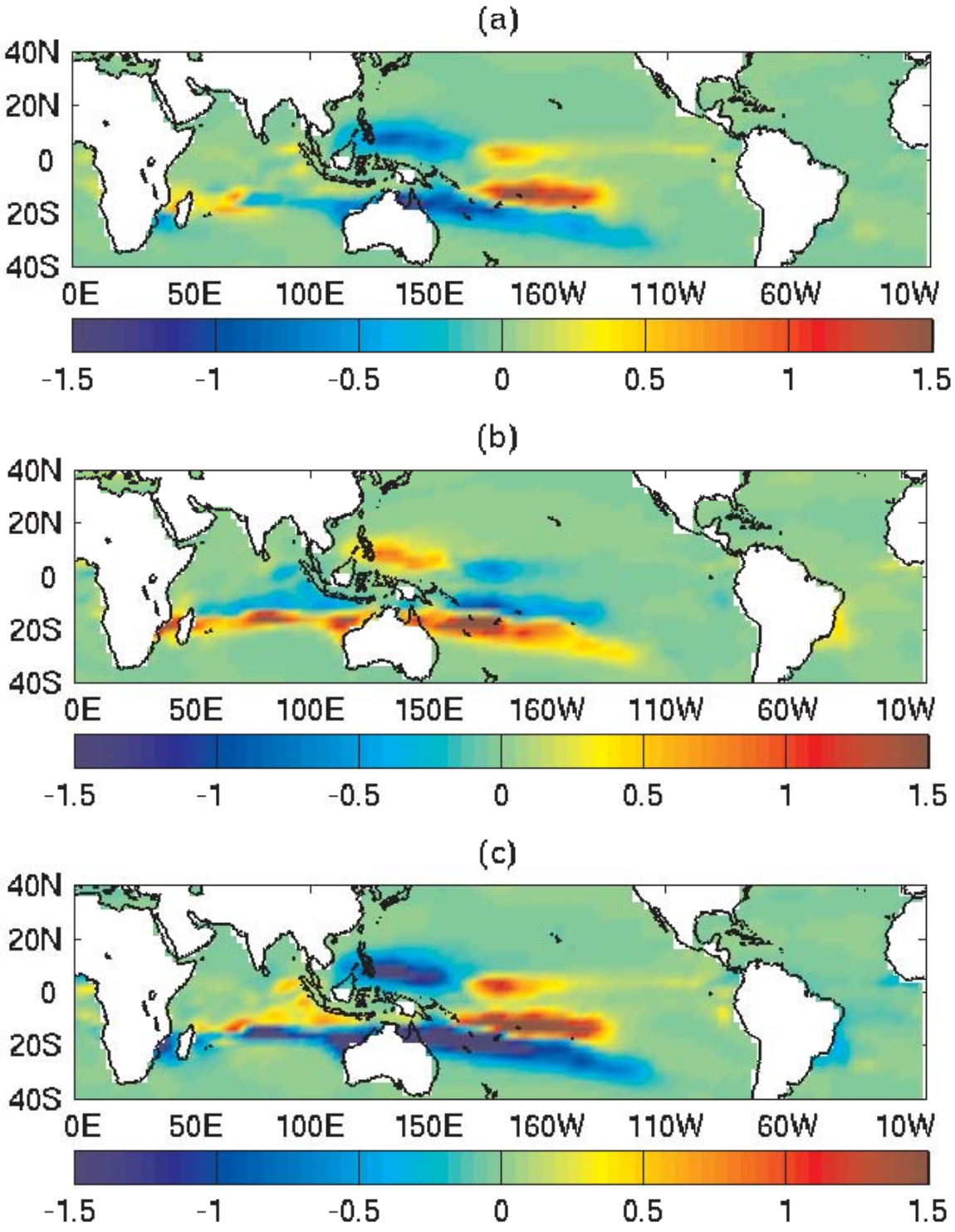

Figure 8: Genesis potential anomalies in JFM (January-March) for (a) El Niño and (b) La Niña years; (c) difference of the anomalies in El Niño and La Niña years.

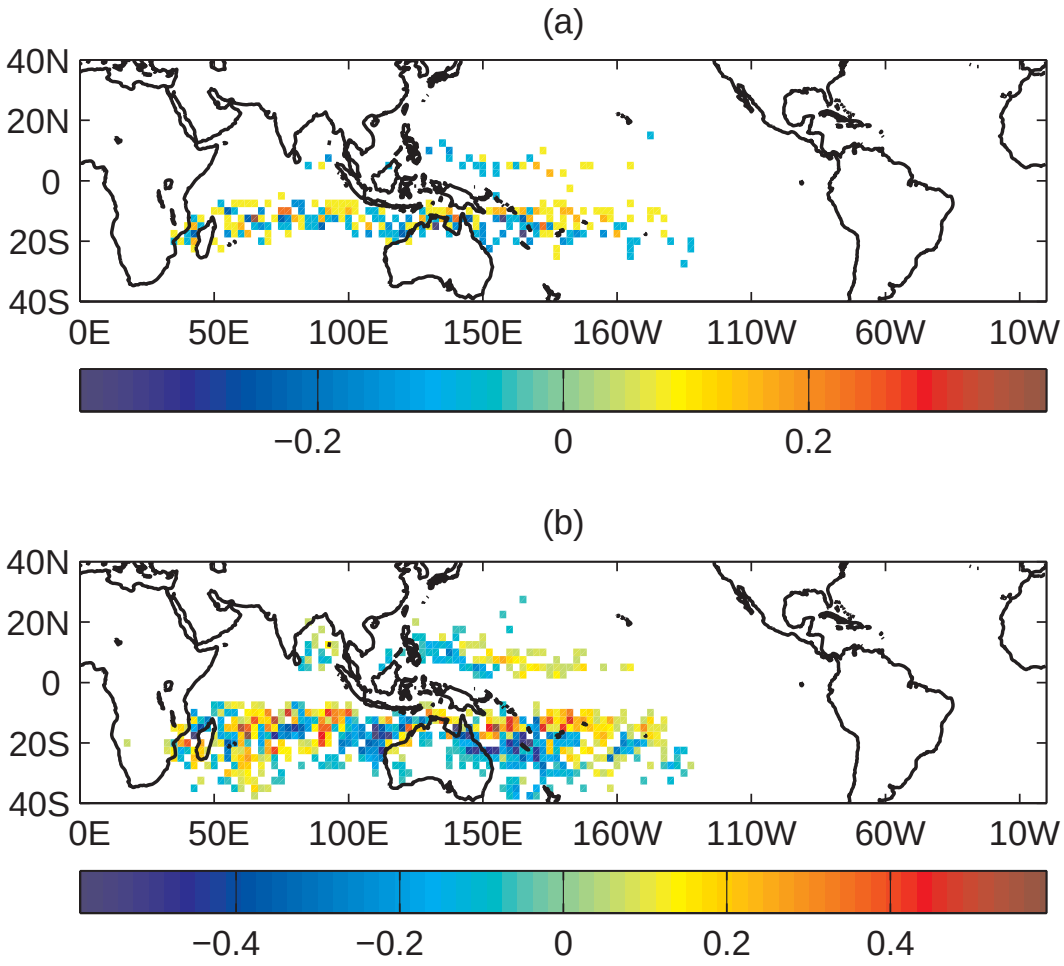

Figure 9: Difference of the anomalies in El Niño and La Niña years for the genesis density (a) and track density (b) in JFM.

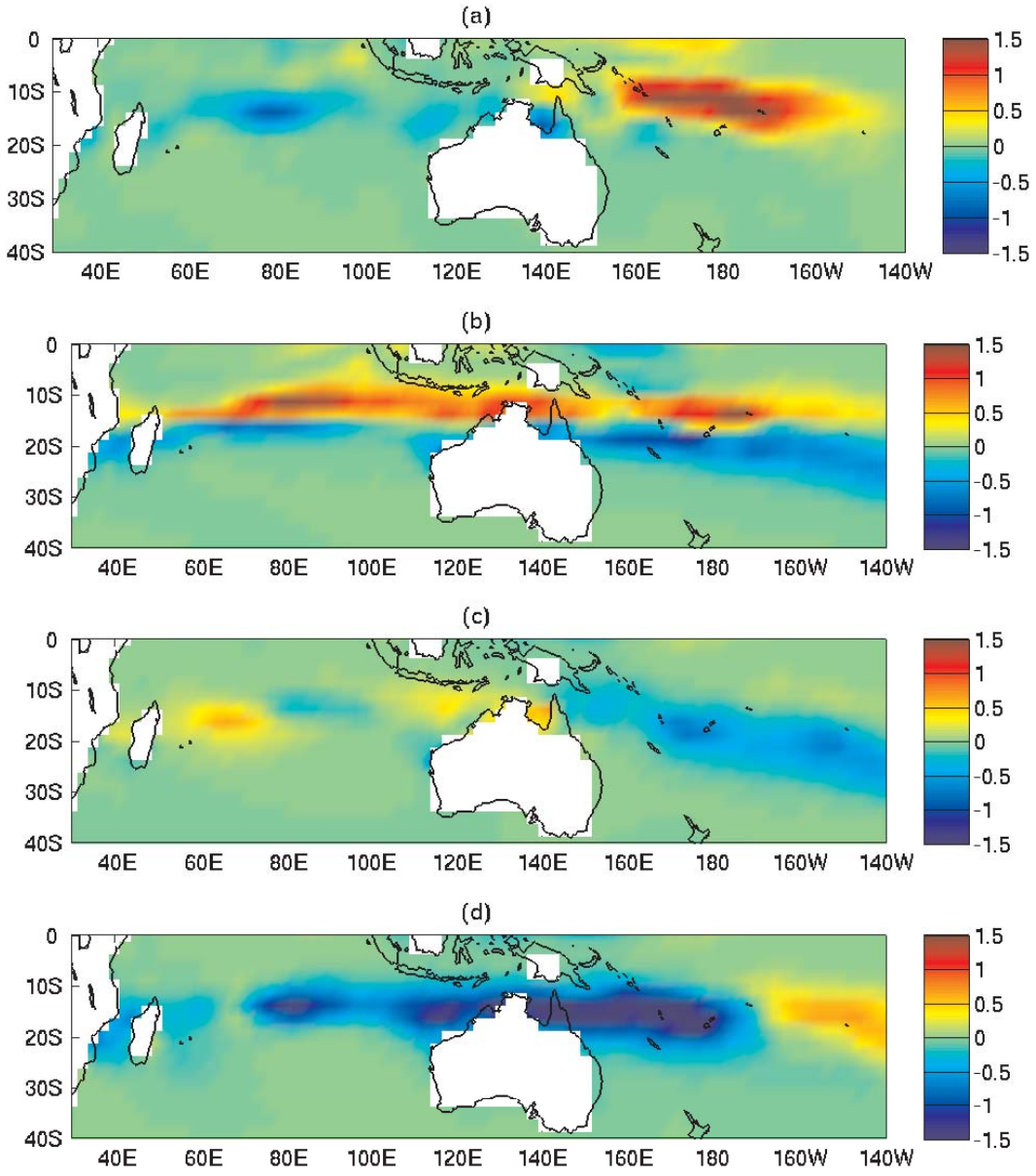

Figure 10: Difference of El Niño and La Niña genesis potential composites in the southern hemisphere in JFM for varying (a) vorticity, (b) vertical wind shear, (c) potential intensity, (d) relative humidity, respectively, with the other variables as climatology.

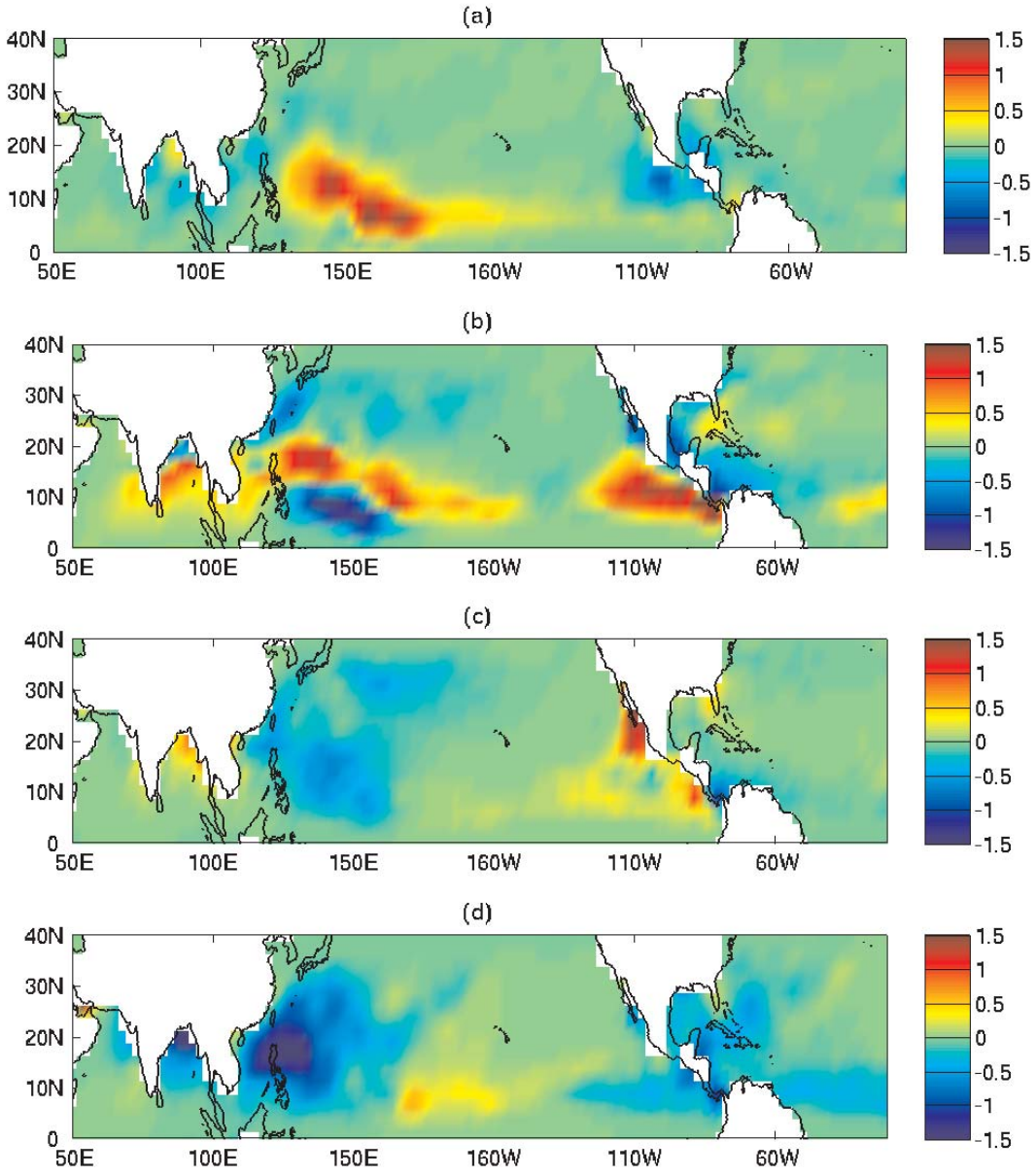

Figure 11: Difference of El Niño and La Niña genesis potential composites in the northern hemisphere in ASO for varying (a) vorticity, (b) vertical wind shear, (c) potential intensity, (d) relative humidity, respectively, with the other variables as climatology.

List of Tables

Table 1: El Niño and La Niña years for JFM (January - March) and ASO (August - October) used in the composites of the genesis potential index in Figs. 6 - 11.

JFM		ASO	
El Niño	La Niña	El Niño	La Niña
1958	1950	1951	1950
1966	1955	1957	1954
1969	1956	1963	1955
1970	1968	1965	1956
1973	1971	1969	1964
1977	1974	1972	1970
1983	1976	1982	1971
1987	1985	1986	1973
1988	1986	1987	1975
1992	1989	1991	1988
1995	1996	1997	1995
1998	1999	2002	1998
2003	2000	2004	1999

Table 2: Correlations of the number of named tropical cyclones and the basin average genesis potential index in the period 1970-2005. The basins are defined by oceanic regions within the following ranges: in the southern hemishere (40°S - 0°), in the northern hemisphere (0° - 40°N); longitudes: South Indian – SI (30°E - 100°E), Australian – AUS (100°E - 180°), South Pacific – SP (180° - 110°W), North Indian – NI (40°E - 100°E), Western North Pacific – WNP (100°E - 180°), Central North Pacific – CNP (180° - 140°W), Eastern North Pacific – ENP (140°W to American coast), Atlantic (American coast to African coast). Twelve three months continuous seasons were used from JFM (January to March) to DJF (December to February). Only shown are seasons and basins in which at least more than 50% of the years there are occurrence of tropical cyclones. Statistical significance was obtained using a two-tailed test, taking into account the auto-correlations of each time-series following Livezey (1983). Bold face (underlined) indicates statistical significance at the 95% (90%) level.

Season	SI	AUS	SP	NI	WNP	CNP	ENP	ATL
JFM	0.23	0.25	0.18	—	0.27	—	—	—
FMA	0.19	0.34	0.25	—	**0.54**	—	—	—
MAM	-0.15	0.35	—	0.18	**0.65**	—	-0.05	—
AMJ	-0.14	0.16	—	0.28	**0.50**	—	0.07	0.11
MJJ	-0.24	—	—	0.37	0.46	—	-0.10	0.29
JJA	—	—	—	0.56	0.29	—	0.00	**0.54**
JAS	—	—	—	—	0.10	0.45	0.26	**0.63**
ASO	0.15	—	—	0.10	0.16	0.60	0.51	**0.60**
SON	0.14	-0.13	—	0.13	0.21	0.63	0.48	0.28
OND	0.17	0.24	—	0.06	**0.45**	—-	0.05	0.28
NDJ	0.36	0.32	**0.42**	0.03	0.33	—	—	—
DJF	0.42	0.29	0.38	—	**0.44**	—	—	—